Progress in the Development of the MISTE Flight Experiment

M. Barmatz, Inseob Hahn and F. Zhong

Jet Propulsion Laboratory, California Institute of Technology, 4800 Oak Grove Drive, Pasadena, CA 91109

(Dated: August 15, 2000)

The MISTE flight experiment plans to measure the specific heat at constant volume, C_V, and isothermal susceptibility, χ_T, near the ^{3}He liquid-gas critical point. Precision ground-based experiments have been performed in the crossover region away from the critical point in preparation for this flight. A new method for precisely determining the critical temperature is being evaluated and will be presented. A sweep electrostriction method was also demonstrated for obtaining the isothermal susceptibility close to the critical point. We have been able to demonstrate that the chemical potential can be obtained from these electrostriction measurements. Pressure versus density measurements along isotherms below the critical temperature were performed to determine the isothermal susceptibility along the coexistence curve. These measurements are compared to susceptibility data obtained along the critical isochore above the transition.

I. INTRODUCTION

The MISTE flight experiment plans to perform heat capacity at constant volume, C_V, isothermal susceptibility, χ_T, and PVT measurements in the same experimental cell near the liquid-gas critical point of ^{3}He. These experiments, performed in a microgravity environment, will provide measurements in the asymptotic region two decades in reduced temperature closer to the transition. The constant-volume heat capacity along the critical isochore and the isothermal susceptibility along the critical isochore and coexistence curve are expected to satisfy the following fluctuation-induced theoretical expressions:

$$C_V^{\pm *} = (T_c\rho_c/P_c)C_V^{\pm} = A_0^{\pm}|t|^{-\alpha}[1 + A_1^{\pm}|t|^{\Delta_s} + ...] + B_{cr} \quad (1)$$

$$\chi_T^{\pm *} = (P_c/\rho_c^2)\chi_T^{\pm} = \Gamma_0^{\pm}|t|^{-\gamma}[1 + \Gamma_1^{\pm}|t|^{\Delta_s} + ...], \quad (2)$$

where $\alpha \simeq 0.11$ and $\gamma \simeq 1.24$ are universal critical exponents and $A_0^{\pm}$ and $\Gamma_0^{\pm}$ are system-dependent critical amplitudes. The superscripts "+" and "–" correspond to positive and negative reduced temperatures $t \equiv (T - T_c)/T_c$, respectively. The isothermal susceptibility along the coexistence curve is given by χ_T^{-*}. The system-dependent critical parameters are T_c, ρ_c, and P_c, and B_{cr} is a constant, fluctuation-induced term. The confluent singularity expansion in the brackets includes an independent universal correction-to-scaling exponent,[1] $\Delta_s = 0.52 \pm 0.02$ and system-dependent amplitudes $A_1^{\pm}$ and $\Gamma_1^{\pm}$. Analytic background terms must also be included in analyzing heat-capacity measurements.

Critical phenomena theories can predict critical exponents and universal amplitude ratios. However, an exact determination of the asymptotic region cannot be made theoretically since the leading critical amplitudes and the amplitudes associated with correction-to-scaling confluent singularities are system dependent. The MISTE flight experiment should permit an accurate determination of the leading system-dependent asymptotic critical amplitudes for ^{3}He. A knowledge of these asymptotic amplitudes will permit a more accurate analysis of crossover measurements farther away from the transition. Ground-based studies are now being performed in the crossover region[2] in preparation for this future flight experiment. The results of some of these studies will be reported in this paper.

II. GROUND–BASED EXPERIMENTS

Ground-based measurements were performed in a flat pancake fluid cell shown in Fig. 1. The cell temperature was measured using a $GdCl_3$ high resolution thermometer (HRT) with a sensitivity of $\sim$ 1 nK near the ^{3}He critical point ($T_c = 3.31$ K). The density sensor was a parallel plate capacitor situated half way between the top and bottom of the cell. The density was determined from the measurement of the dielectric constant using the Clausius-Mossotti equation. A Straty-Adams type pressure sensor was also situated at the midplane of the cell. This sensor consisted of a parallel plate capacitor with one plate attached to a flexible diaphragm that sensed pressure changes in the cell. This experimental configuration has the advantage that pressure, density, and temperature data can be continuously obtained in the same cell while heat capacity and susceptibility measurements were being performed.

The isothermal susceptibility, $\chi_T = \rho(\partial\rho/\partial P)_T$, was measured along isotherms both above and below the crit-

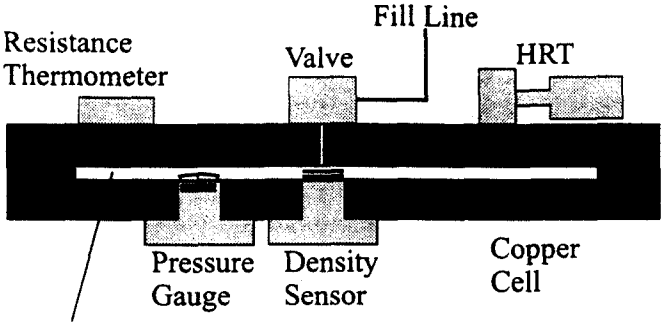

FIG. 1: Schematic of ground-based cell for measuring heat capacity and susceptibility.

ical temperature. This was achieved by initially overfilling the cell and then slowly removing fluid from the cell and measuring the density and pressure as a function of time. Susceptibility data were obtained from the slope of P versus ρ curves in the reduced temperature range of $6 \times 10^{-5} < |t| < 10^{-1}$. As the critical temperature is approached, the susceptibility maximum versus ρ approaches the critical density, ρ_c. After completing the susceptibility measurements, the low temperature valve was closed at the critical density. Heat-capacity measurements were then performed using a pulse technique in the single and two-phase regions over the range $5 \times 10^{-4} < |t| < 10^{-1}$. Drift heat-capacity measurements were also performed close to the transition. These new C_V and χ_T data agreed with earlier measurements from Horst Meyer's group[3–6] over the same temperature range.

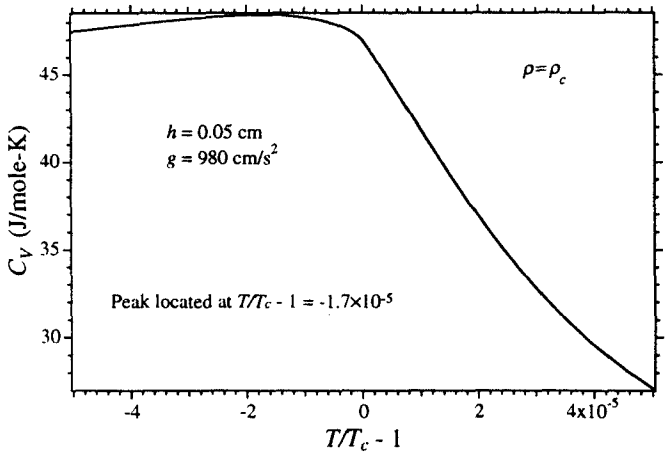

FIG. 2: Restricted cubic model prediction for the ^{3}He heat capacity in a 0.05 cm high cell along the critical isochore in 1g. A change in slope is predicted at the transition temperature.

III. DETERMINATION OF THE CRITICAL TEMPERATURE

In order to successfully analyze experimental measurements near a critical point, it is important to determine the critical temperature as precisely as possible. There are several methods for finding T_c. One approach is to have T_c be a fitting parameter when analyzing data. However, the accuracy of the resultant T_c will depend on the model chosen and closeness of the data to the transition. One can also attempt to use some characteristic signature of the transition. For example, it is known that the time constant for equilibrium in performing heat capacity measurements is much greater in the two phase region. Unfortunately, in ground-based measurements, the gravity induced density gradient smears out this sudden change near the transition. We have recently been investigating a new slow drift heat capacity approach for determining the transition temperature. Figure 2 shows the restricted cubic model[7] prediction for the ^{3}He heat capacity in our 0.05 cm high cell along the critical isochore in 1g. In a gravitational field, theory predicts an experimentally measurable change in the temperature derivative of C_V at T_c with a heat capacity maximum occurring in the two-phase region. We see a change in slope occurring at the transition with the peak value located at a reduced temperature of $t \approx -1.7 \times 10^{-5}$ below T_c. An example of our experimental measurements performed during a slow drift down through the transition is shown in Fig. 3. There is a kink in the data that we associated with the transition temperature T_c. The transition temperature can be determined to better than $\pm 15 \mu$K. The peak in these data is at $t \approx -2.3 \times 10^{-5}$, which is close to the theoretically predicted value. Additional measurements are planned at even slower drift rates to make sure we have this level of reproducibility in determining T_c.

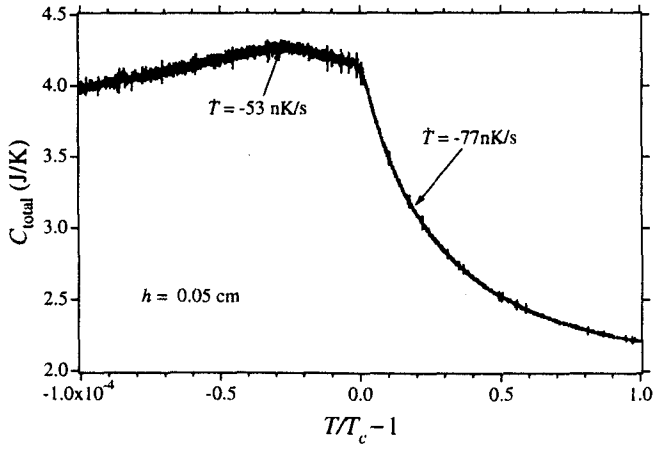

FIG. 3: Experimental drift measurements of the ^{3}He heat capacity along the critical isochore in 1g.

IV. CHEMICAL POTENTIAL

An electrostriction technique was previously developed[8] to perform susceptibility measurements within $t < 10^{-4}$. This technique is based on the fact that an electric field gradient can produce a pressure gradient within a dielectric fluid ($\delta P \propto E^2$) that in turn induces a density change. Our approach is to apply a dc voltage across a parallel plate capacitor to produce a uniform electric field within the density sensor capacitor gap. The density change $\delta\rho$ is obtained at several voltages and $\delta\rho/\delta P$ is determined in the limit of zero voltage. We have been evaluating drift electrostriction measurements using a fixed dc voltage across the gap. Figure 4 shows measurements of the density change between the applied dc voltage and zero dc voltage. The drift rates were $\approx -4 \times 10^{-4}$ K/hr. The susceptibility at any given temperature can be obtained by extrapolating the density values obtained from these curves to zero dc voltage. We also performed equilibrium measurements, shown by symbols, at a few reduced temperatures to see if this drift rate was slow enough. Good agreement was obtained between the drift and equilibrium measurements down to about a reduced temperature of $t = 5 \times 10^{-5}$. The MISTE flight experiment plans to reach a reduced temperature of 10^{-6} that will require even slower drift rates.

We have realized that this electrostriction technique can be used to conveniently determine the chemical potential difference $\mu - \mu_c$. This conclusion can be seen as follows. Scaling theory predicts that, in the asymptotic region, the chemical potential difference from its critical value can be scaled by a universal function h

$$(\mu^*(\rho,T) - \mu^*(\rho_c,T))/(\Delta\rho|\Delta\rho|^{\delta-1}) = Dh(x/x_0) \quad (3)$$

where $\mu^* = (\rho_c/P_c)\mu$, $x = t/(|\Delta\rho|)^{1/\beta}$, and $x_0 = 1/B_0^{1/\beta}$.

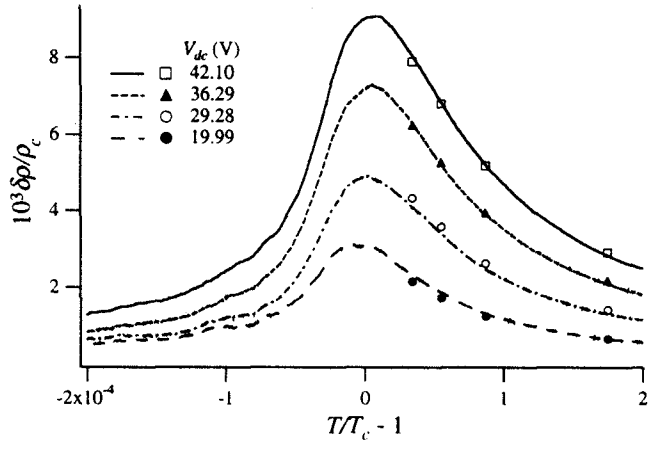

FIG. 4: Density change versus temperature for electrostriction drift (lines) and equilibrium (symbols) measurements at various constant applied dc bias voltages.

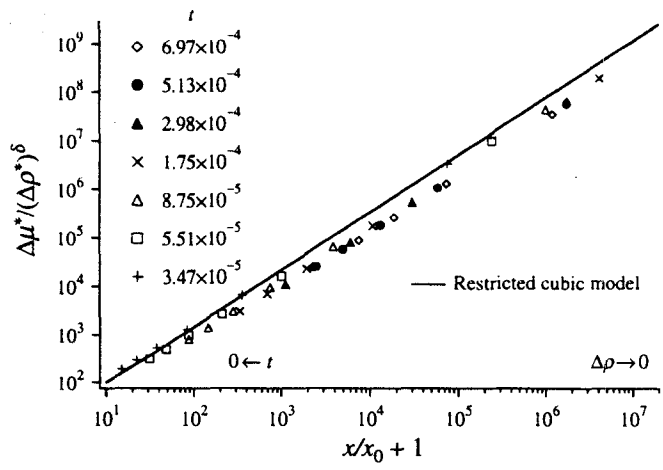

FIG. 5: Comparison of electrostriction measurements to theoretically predicted universal curve for the chemical potential.

The reduced density $\Delta\rho \equiv \rho/\rho_c - 1$, β is the critical exponent that defines the shape of the coexistence curve, and D is the asymptotic critical amplitude associated with the divergence of the pressure with density along the critical isotherm. The chemical potential can be written as $d\mu = -sdT + dP/\rho$. Under isothermal conditions the integration of this expression reduces to

$$\mu(\rho_2,T) - \mu(\rho_1,T) = \int_{P(\rho_1,T)}^{P(\rho_2,T)} dP/\rho. \quad (4)$$

Since the pressure gradient induced by an electric field gradient is given by

$$\nabla P = (\epsilon_0\rho/2)\nabla(E^2(\partial\epsilon/\partial\rho)), \quad (5)$$

we can write the chemical potential difference between two densities, Eq. (4), as

$$\mu(\rho_2,T) - \mu(\rho_1,T) = (3\epsilon_0\zeta_c\rho_c/2(\rho_c - \zeta_c\rho_2)^2)E^2, \quad (6)$$

where $\zeta_c = 4\pi\alpha'/3$ with α' being the polarizability of the fluid. By setting the lower ambient density equal to the critical density we obtain the following expression for the chemical potential universal curve

$$Dh(x/x_0) = (3\epsilon_0\zeta_c\rho_c/2(\rho_c - \zeta_c\rho_2)^2)(E^2/(\Delta\rho)^\delta). \quad (7)$$

The right side of this equation can be determined experimentally since we measure the density ρ_2 and can calculate $\Delta\rho$ and the electric field. Figure 5 is a plot of the chemical potential universal curve. The solid line is the prediction from the restricted cubic model and the data points come from equilibrium electrostriction measurements at various temperatures. We do not expect

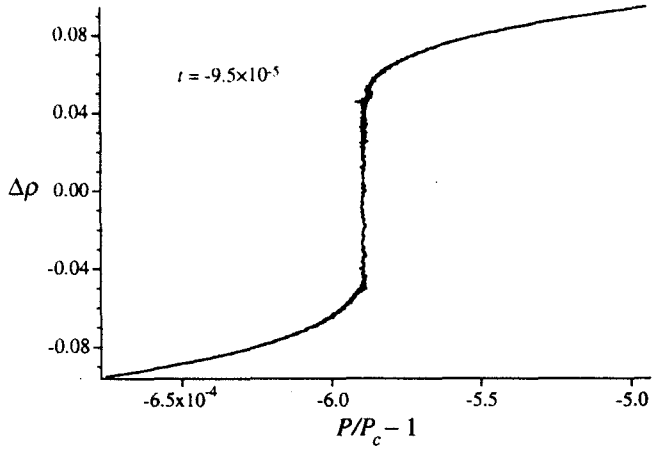

FIG. 6: Pressure versus density along an isotherm below T_c

to have a good fit between theory and experiment since most of the data points are not in the asymptotic region. In this plot the asymptotic region is approached as t and $\Delta\rho \rightarrow 0$. However, we anticipate a much more stringent test of this scaling theory prediction coming from the MISTE flight experiment where measurements will be performed much closer to the transition.

V. SUSCEPTIBILITY MEASUREMENTS

The isothermal susceptibility along the coexistence curve can also be obtained from pressure versus density measurements as stated above. Figure 6 shows an example of P versus ρ measurements at a reduced temperature of $t = -9.5 \times 10^{-5}$. The break in $(\partial\rho/\partial P)_T$ at a reduced density $\Delta\rho \approx 5\%$ indicates the onset of the two-phase region inwhich the pressure remains constant until the gas side of the coexistence curve is reached at $\Delta\rho \approx -5\%$. The susceptibility at the coexistence curve is obtained from the slope of this curve as it enters and exits the two-phase region. The coexistence curve densities at this temperature can also be determine from such breaks in the slope to within $\pm$ 0.1%. This method for determining the susceptibility and coexistence curve will become less precise as the transition is approached since the change in slope will be less pronounced.

The experimentally determined susceptibility along the critical isochore and coexistence curve are shown in Fig. 7. Earlier measurements from Wallace and Meyer[3] and Pittman, Doiron, and Meyer[4] have also been included. The MISTE measurements along the coexistence curve extend over a decade closer to the transition than the earlier data. We see good agreement between the various measurements in the regions of overlap. The susceptibility along the coexistence curve and critical isochore seems to have the same slope in this log-log plot, with the coexistence curve susceptibility having a smaller magnitude. To estimate the difference in magnitude between the susceptibility data above and below the transition, the critical isochore data were divided by 3.7 to approximately overlap the coexistence curve data. This is the same value used by Wallace and Meyer in their earlier work[3]. This factor of 3.7 corresponds to an effective ratio of the critical amplitudes $(\Gamma_0^+/\Gamma_0^-)_{eff}$ in the crossover region. These normalized data are shown in Fig. 8. It is surprising to see that all the data sets are consistent with each other over three decades in reduced temperature. Critical phenomena theories[9] predict a ratio $\Gamma_0^+/\Gamma_0^- = 4.95$ in the asymptotic region. Since most of these ground-based susceptibility data are outside the asymptotic region, additional measurements

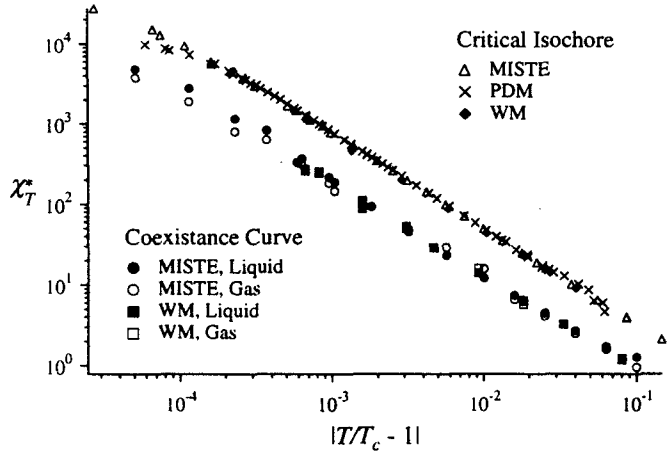

FIG. 7: Susceptibility measurements along the critical isochore above T_c and along the coexistence curve below T_c. Also included are the data from Pittman, Doiron and Meyer (PDM) and Wallace and Meyer (WM).

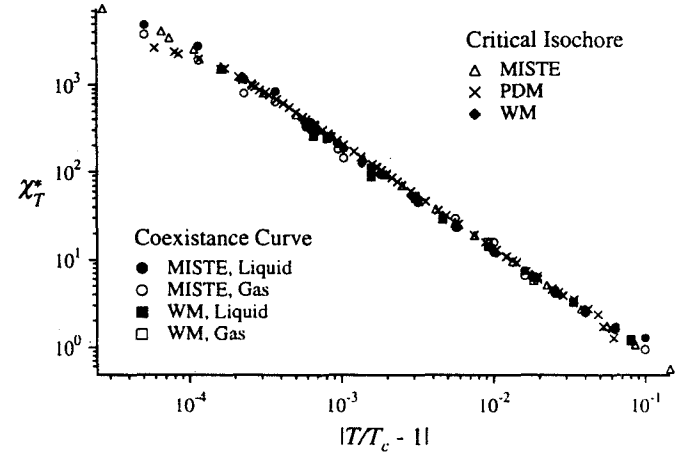

FIG. 8: Normalized susceptibility measurements above and below T_c. Also included are the data from Pittman, Doiron, and Meyer (PDM) and Wallace and Meyer (WM).

from the MISTE flight experiment are needed closer to the transition to test this asymptotic theoretical prediction and to obtaining a better understanding of the observed crossover behavior.

VI. FUTURE STUDIES

The recent heat capacity and susceptibility measurements need to be analyzed using accurate theoretical crossover models in order to obtain a better understanding of thermodynamic behavior farther away from the transition. We began this process by analyzing our susceptibility data along the critical isochore above the transition using a field theoretical Renormalization-Group ϕ^4 model[10] recently adapted to the $O(1)$ universality class[11]. The results of this initial study[12] suggested that the ϕ^4 model would be a useful tool to investigate thermodynamic quantities measured along the critical isochore and coexistence curve. More recently, we have used this model to successfully analyze our heat capacity data along the critical isochore[13]. The MISTE susceptibility and heat-capacity data have also been analyzed successfully using a new crossover parametric equation-of-state[13]. Further analyses of thermodynamic measurements throughout the critical region are planned using both the crossover parametric equation-of-state and ϕ^4 models.

ACKNOWLEDGMENTS

The research described in this article was carried out at the Jet Propulsion Laboratory, California Institute of Technology, under contract with the National Aeronautics and Space Administration. The authors are indebted to Dr. M. Weilert for supporting the experimental measurements and data analysis.

REFERENCES

[1] R. Guida and J. Zinn-Justin, J. Phys. A: Math. Gen. **31**, 8103 (1998).
[2] M. Barmatz, *MISTE Science Requirements Document*, Tech. Rep. JPL D-17083, JPL (1999).
[3] B. Wallace and H. Meyer, Phys. Rev. A **5**, 953 (1972).
[4] C. Pittman, T. Doiron, and H. Meyer, Phys. Rev. B **20**, 3678 (1979).
[5] C. C. Agosta, S. Wang, L. H. Cohen, and H. Meyer, J. Low Temp. Phys. **67**, 237 (1987).
[6] R. G. Brown and H. Meyer, Phys. Rev. A **6**, 364 (1972).
[7] F. Zhong and H. Meyer, Phys. Rev. E **51**, 3223 (1995).
[8] M. Barmatz, F. Zhong, and I. Hahn, Physica **B 284-288**, 206 (2000).
[9] M. E. Fisher and S.-Y. Zinn, J. Phys. A: Math. Gen. **31**, L629 (1998).
[10] R. Schloms and V. Dohm, Nuclear Physics **B328**, 639 (1989).
[11] R. Haussmann (private communication).
[12] I. Hahn, F. Zhong, M. Barmatz, R. Haussmann, and J. Rudnick (to be published).
[13] M. Barmatz, I. Hahn, F. Zhong, M. A. Anisimov, and V. A. Vaktang (to be published).